Self-mixing differential vibrometer based on electronic channel subtraction

Silvano Donati, Michele Norgia, and Guido Giuliani

An instrument for noncontact measurement of differential vibrations is developed, based on the self-mixing interferometer. As no reference arm is available in the self-mixing configuration, the differential mode is obtained by electronic subtraction of signals from two (nominally equal) vibrometer channels, taking advantage that channels are servo stabilized and thus insensitive to speckle and other sources of amplitude fluctuation. We show that electronic subtraction is nearly as effective as field superposition. Common-mode suppression is 25–30 dB, the dynamic range (amplitude) is in excess of 100 μm, and the minimum measurable (differential) amplitude is 20 nm on a $B = 10$ kHz bandwidth. The instrument has been used to measure vibrations of two metal samples kept in contact, revealing the hysteresis cycle in the microslip and gross-slip regimes, which are of interest in the study of friction induced vibration damping of gas turbine blades for aircraft applications.

OCIS codes: 120.3930, 120.3180, 280.3420, 030.6140, 120.7280.

1. Introduction

Laser vibrometers are well-known interferometric instruments[1–3] for the measurement of minute vibration of a remote target without physical contact and with very good sensitivity. In recent years, a technique called self-mixing interferometry (SMI) or optical feedback interferometry[1,3] has gained acceptance, thanks to its simple optical setup, requiring just a diode laser (DL) as the optical source and a focusing lens. In a self-mixing configuration, light from a DL is focused on the remote target, and a fraction of the backscattered light is allowed to re-enter the SL cavity where it is coherently mixed with the lasing field. This generates a modulation of the emitted power in the form of an interferometric signal carrying the phase information related to the path length of light from the DL to the target and back. The interferometric signal can be detected by the monitor photodiode (PD) usually already available in the DL package. SMI is a single-channel configuration, does not require a reference arm, and has a minimum optical part count. It has been successfully demonstrated in a variety of measurement applications, such as displacement,[3–5] absolute distance,[6] vibrations,[7,8] and angles.[9]

SMI readily measures vibrations of the target with good sensitivity, but, because of the inherent single-channel structure lacking a reference path, a differential measurement of vibrations on two distinct points is not possible, at least in the basic form. We show how to circumvent this limitation of SMI. Because SMI is single channel and so simple, we may as well duplicate it and perform the difference of the outputs of the two-channel structure, provided we are able to maintain the two channels stably and well tracked. This is ensured by the feedback loop action of the half-fringe stabilization loop. We show that this electrical subtraction is indeed viable and allows us to achieve sensitivity comparable to that of a conventional, referenced interferometric configuration.

The case of interest for our application was the characterization of the contact between two vibrating bodies, requiring the measurement of small amplitude differential displacement. The measurement has to deal with the energy dissipated by the contact friction forces and hence helps to understand the dynamics of vibration damping.[10] In particular, the relationship between tangential forces in the contact point and the relative displacement is linear when the amplitude of vibration is small, whereas it exhibits hysteresis at large amplitude as the tangential

S. Donati (silvano.donati@unipv.it), M. Norgia, and G. Giuliani (guido.giuliani@unipv.it) were with the Dipartimento di Elettronica, Universitá di Pavia, Via Ferrata 1, Pavia I-27100, Italy. M. Norgia is now with the Dipartimento di Elettronica e Informazione, Politecnico di Milano, Via Ponzio 34-5, Milan I-20133, Italy.

Received 4 November 2005; revised 20 February 2006; accepted 28 April 2006; posted 23 May 2006 (Doc. ID 65779).

0003-6935/06/287264-05$15.00/0

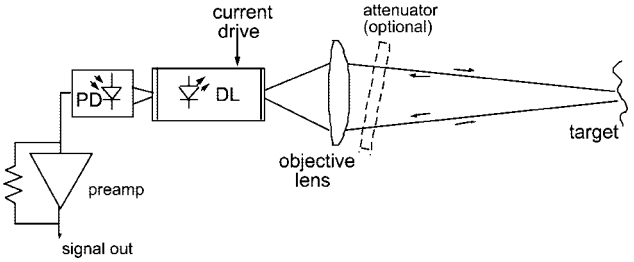

Fig. 1. Schematic of the optical head: an 825 nm semiconductor laser (DL) is used as the source, and its monitor photodiode (PD) is mounted internally in the package, behind the rear mirror, is the detector of the SMI. An anamorphic objective lens is used to collimate the beam and direct it onto the diffusing target. A transimpedance amplifier brings the photocurrent to a level large enough for subsequent signal processing.

force approaches a limiting value and the contact enters the gross-slip regime.

Friction damping is fundamental in quenching vibration in gas turbine blades, in order to improve endurance and aircraft safety. Usually, damping is provided by underplatform dampers or by shroud-type contacts, which exploit friction at the contact to dissipate the vibration energy.[10,11] Modeling the contact regime requires the measurement of hysteresis cycles for different contact geometry and material properties. Also in favor of the optical approach, contact materials working in turbine blades become heated up to high temperatures, reaching 800 °C.

A test rig was developed to characterize friction hysteresis.[12] The aim of measurement is to plot in real time and, simultaneously, the tangential contact force (measured by a piezoelectric force transducer) and the differential displacement. The rig consists of a beam carrying one specimen, to bring it in contact with a second specimen held in position in a special fixture. The two specimens are loaded against each other in the normal contact direction by a constant load. When the beam is vibrated, the specimen attached to it rubs against the other, developing the contact hysteresis.

The driving force is swept in frequency typically from a few hertz to hundreds of hertz, producing common-mode displacements up to 50–100 μm. The differential vibration amplitude is up to 20–30 μm, and this quantity shall be measured with an accuracy of approximately 20 nm (for contact parameters extraction). The displacement point is very close to the contact surface, thus ruling out measurement approaches based on capacitive or eddy current.

2. Differential Self-Mixing Vibrometer

The optical head of each channel is shown in Fig. 1. Light from a single longitudinal mode Fabry–Perot DL is focused onto the target through an objective lens. Backscattered light is focused back into the laser and modulates the cavity field. The monitor PD, on the rear laser mirror, collects a fraction of the SMI signal, which is found[1–4] as

$$P(\phi) = P_0[1 + mF(\phi)], \qquad (1)$$

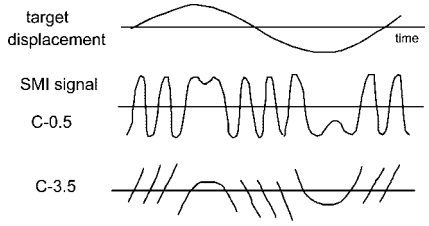

Fig. 2. Driving the target with a sine wave, the SMI signal resembles the normal (Bessel-like) interferometric signal at low injection levels ($C \approx 0.5$). At increased C factors, the signal is progressively distorted and then becomes a sawtoothlike waveform (bottom, $C \approx 3.5$).

where P_0 is the power emitted by the unperturbed SL, $F(\phi)$, is a periodic function of phase $\phi = 2\,ks$, where $k = 2\pi/\lambda$, and m is the modulation index (typically $\approx 10^{-6}$ to 10^{-3} in most cases). The exact shape of the interferometric function $F(\phi)$ depends on feedback parameter C, which, in turn, depends on parameters of the laser and also on the target distance s and the power reflectivity of target R_{eff} (see Refs. 3 and 4 for details).

It is important to note that for the weak feedback ($C \ll 1$), the function $F(\phi)$ is a cosine, just as the usual interferometric waveform, whereas for the moderate feedback (i.e., $C \approx 1$), the function $F(\phi)$ becomes sawtoothlike (Fig. 2) and this allows for the discrimination of the sign of target displacement, as explained in Refs. 3–6. From this interferometric signal, the vibration amplitude can be retrieved with a $\lambda/2$ accuracy just by counting the number of fringes.

To improve resolution further, a feedback-loop technique has been developed so that the minimum detectable vibration is ultimately limited by noise rather than by the $\lambda/2$ quantization of fringe counting. The technique has been presented in Ref. 7 to which the reader is directed for the details. Here, we just discuss those features that are crucial for understanding how precise the difference of vibration signals can be, i.e., to get a good common-mode suppression.

Basically, we construct a servo loop around the interferometer (Fig. 3) by feeding back an error signal to the experiment, so as to keep the output phase read

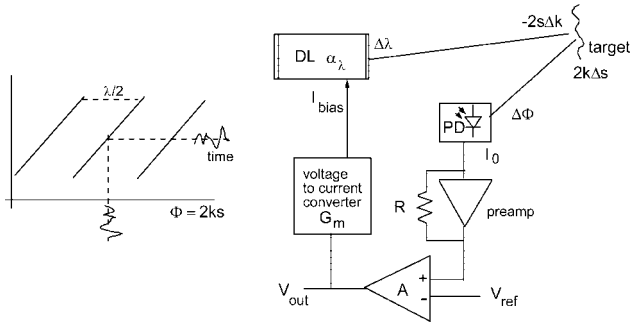

Fig. 3. Working at $C > 1$, the SMI can be stabilized at half-fringe (left) by a simple feedback loop (right) feeding back to the bias current of the DL from the amplified SMI signal.

by the SMI constant. In the experiment, the total phase variation $\Delta\Phi = \Delta(2ks) = 0$ is nulled dynamically by changing the wavelength, so that $2k\Delta s + 2s\Delta k = 0$ or, being $\Delta k/k = -\Delta\lambda/\lambda$, with $\Delta\lambda = \lambda\Delta s/s$. The wavelength change is obtained by a bias-current change, as $\Delta I_{\text{bias}} = (1/\alpha_\lambda)\Delta\lambda$, α_λ being a coefficient specific of the DL. Additionally, phase $\Delta\Phi$ produces a signal ΔV, at the PD output, given by

$$\Delta V = RI_0 \sin \Delta\Phi \approx RI_0\Delta\Phi, \tag{2}$$

here, R is the transresistance of the preamplifier stage, and I_0 is the peak SMI component of total photocurrent signal, or explicitly,

$$I_{\text{ph}} = I_{\text{ph0}} + I_0 \cos \Delta\Phi. \tag{3}$$

After a gain A in the main amplifier, a signal error is developed that is fed to the current driver of the laser as

$$\Delta I_{\text{bias}} = G_m A \Delta V, \tag{4}$$

G_m being the transconductance of the driver. Collecting the terms, we can see that the loop has a total gain given by

$$A_{\text{loop}} = 2ks(\alpha_\lambda/\lambda)I_0 G_m A R, \tag{5}$$

whereas from displacement signal Δs to the output ΔV of the main amplifier, we get a transfer factor given by

$$\Delta V = [\alpha_\lambda G_m]^{-1}\Delta s(\lambda/s). \tag{6}$$

Now, the crucial point is that ΔV depends on Δs through a factor $[\alpha_\lambda G_m]^{-1}(\lambda/s)$, which does not contain the signal power nor its fluctuations, including those due to the speckle statistics introduced by the diffusing target. Indeed, as the zeroing effect shares the same channel as the displacement signal, any dependence from the transfer factors of the common path is canceled out.

Additionally, if we set the reference level in the amplifier at half-fringe amplitude, this level of the signal will be kept constant by the feedback loop, any disturbances being decreased by A_{loop}. In the same way, the dynamic range will no more be limited to $\lambda/2$ as in a normal interferometer, rather it will be increased to $A_{\text{loop}}(\lambda/2)$ by virtue of the feedback effect, as already shown in Ref. 7 Also, the linearity error caused by the sin Φ dependence of the fringe signal is decreased by the loop gain A_{loop}. All these effects are consequences of the feedback loop action, as it is well known from feedback control theory.

Concerning speckle pattern statistics, certainly there are fluctuations in the photodetected signal I_{ph} as the spot on the target is moved from point to point. Yet the signal $\Delta V = RI_0\Delta\Phi$ remains constant because of the feedback action. Stated in other terms, upon aiming the beam on the target we find bright and dark speckles with high and low values of I_{ph} and I_0. The corresponding A_{loop} gain varies accordingly, but not the ΔV. Of course, bright speckles are still preferable, because they provide us with the largest value of A_{loop} for linearity, bandwidth, and dynamic range improvement.

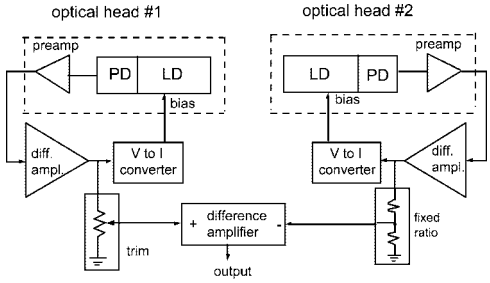

Fig. 4. Block scheme of the self-mixing differential vibrometer based on the electronic subtraction of output signals of two nominally identical channels.

All the data presented below are for the favorable condition of a fairly bright speckle (say ≈2–3 times the average intensity). This condition corresponds to achieving a loop gain of $A_{\text{loop}} \approx 500$. In the practical operation of the instrument, such a bright speckle is readily found by slightly deflecting the laser spot on the target while watching the amplitude I_{ph} so as to find the desired large value.

The block scheme of the SMI differential vibrometer is shown in Fig. 4. Each channel is just an optical head with the LD, a monitor PD backed by the transimpedance amplifier, a difference amplifier, and a current generator feeding the LD.

The output signals of the two channels are subtracted in a difference amplifier (Fig. 4), after the amplitude of one is trimmed to allow for a small (typically ±10%) correction of relative amplitudes. The trimming operation is performed while the light beams of the two channels are aimed to the same position on the target (see Fig. 5) and the target is excited to vibrate to large amplitude (typically 100 μm). The residual amplitude of the difference signal after trimming is approximately 0.15–0.25 μm, or a factor of 400–650 of suppression of the common-mode vibration (or displacement) is achieved.

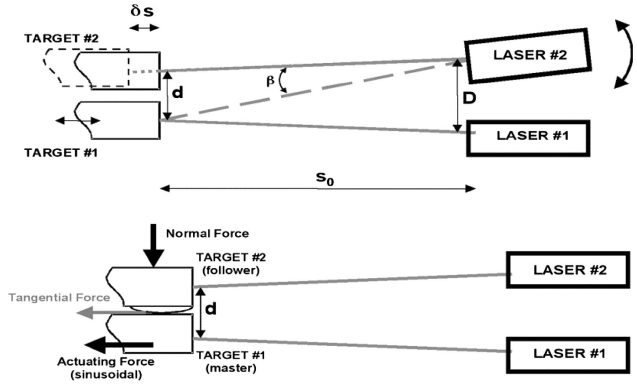

Fig. 5. Top, geometric arrangement of the two optical heads and targets, showing the laser beams in normal operation (solid lines) and during calibration (dashed lines). Bottom, arrangement of the forces applied to the rig assembly carrying the two beadlike targets.

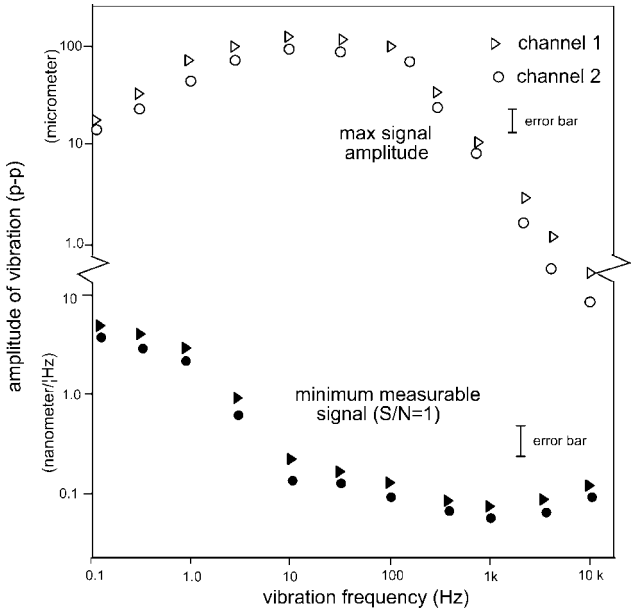

Fig. 6. Maximum measurable peak-to-peak vibration amplitude for the two individual vibrometer channels as a function of frequency, and minimum detectable signal (at $S/N = 1$). Measurements are relative to a white paper surface, placed at a 40 cm distance from the optical heads.

The initial matching of performance of the two channels is good, despite the differences in the parameters of the two DL samples, once again because of the feedback mechanism of the servo loop. In Fig. 6 we plot, as a function of excitation frequency, the maximum signal amplitude handled by both channels before exiting from the fringe and the minimum measurable signal (at a signal-to-noise ratio of 1). The data are quite similar for the two channels and differ by about $\pm 10\%$ in most cases.

After subtraction of the channel output signals, the difference signal has a maximum swing practically equal to the single channel (provided each channel does not exceed its maximum), or up to 100 μm in the frequency range of 5–200 Hz. Here, the roll-off at high frequency is due to the cutoff of the loop gain.

The minimum amplitude of the measurable signal is approximately 200 pm/$\sqrt{\text{Hz}}$ in the range of 10–2000 Hz, and thus in a $B = 100$ Hz bandwidth around the excitation frequency, we can theoretically achieve a minimum detectable signal of $200 \times \sqrt{100} = 2$ nm (at a signal-to-noise ratio of 1). However, as the common-mode vibration is suppressed by about 500, when the common mode is large, e.g., has an ~100 μm amplitude filling the full dynamic range, the minimum measurable signal is limited by the difference error to approximately 200 nm. The noise limit prevails when the common-mode amplitudes are small, i.e., less than or equal to $2\ \text{nm} \times 500 = 1\ \mu\text{m}$ (at a signal-to-noise ratio of 1 and $B = 100$ Hz). All the above data are for operation on a normal diffusing target, for example, plain white paper, on a medium-to-bright speckle.

About the trimming operation, it was found that the best way to minimize the difference is to tilt only one beam, bringing it to be superposed on the other beam at the target location (Fig. 5). This procedure introduces a negligible error in the ratio of voltage to displacement $\Re = \Delta V/\Delta s = [\alpha_\lambda G_m]^{-1}(\lambda/s)$, because the angle β (Fig. 5, top) is small. Indeed, it is $\delta\Re/\Re_0 = 1 - \cos\beta = 1 - \cos(d/s) = 2.8 \times 10^{-5}$, when we assume $s = 0.4$ m and $d = 3$ mm. On the contrary, the offset δs of the two target distances can produce a sizable error, being $\delta\Re/\Re_0 = -\delta s/s = 10^{-3}$ for $s = 0.4$ m and $\delta s = 400$ μm. Thus we have to check the distance s and $s + \delta s$ of the two targets, or we shall be prepared to tolerate a decrease of the common-mode rejection factor. (In practice, by retrimming the gain as indicated in Fig. 4, we can compensate for a $\delta s/s$ error up to a few percent.)

Fig. 7. Picture of the assembled differential vibrometer.

3. Measurements

The instrument (whose prototype is shown in Fig. 7) has been tested in the field by looking at the differential vibration generated in the mechanical experimental test rig set up at the Department of Mechanics, Politecnico di Torino. In this experiment, the two laser beams are aimed at the free surface of two steel samples that are put in contact (as shown in Fig. 5, bottom). The master sample has a flat contact surface and is driven by a sinusoidal force. The follower sample has a spherical contact surface, and it is subject to a force perpendicular to the contact. Due to friction, a tangential force is generated at the contact between the two samples, and this force, acting on the follower sample, is measured by a separate force transducer (a quartz accelerometer). Our aim was to simultaneously measure the tangential force and the differential vibration of the two samples. When the actuating force is small or the normal force is large, microslip of the contact occurs, and the differential vibration is small, generally below 2–4 μm. As soon as the actuating force is sufficiently large to overcome the static friction, gross slip occurs, with much larger differential vibration.

Figure 8(a) shows an example of the acquired waveforms for the tangential force and the differential vibration for the gross-slip regime. Because of the nonlinearity in the magnetic actuator used in the experiment, the waveform of applied force deviates from a pure sinusoid at the working frequency of

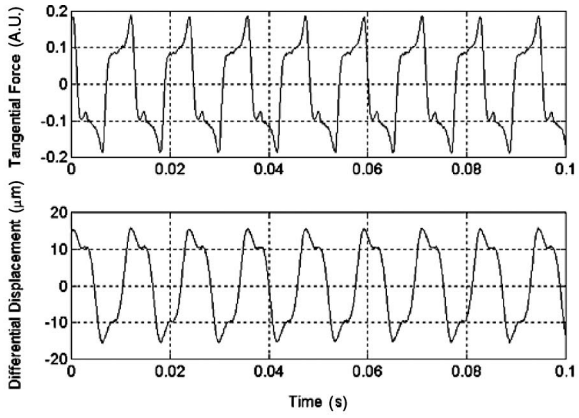

(a)

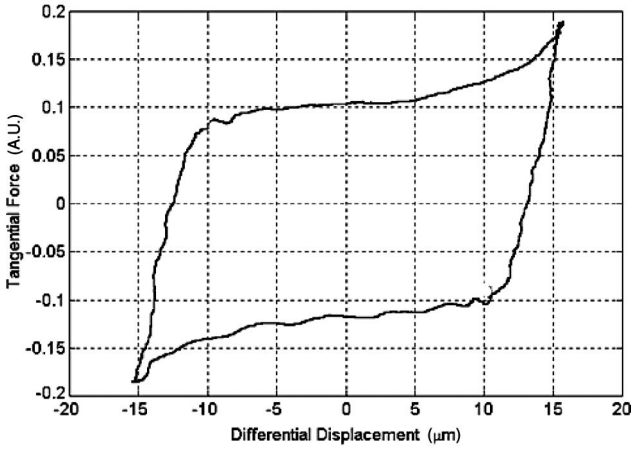

(b)

Fig. 8. (a) Time-domain traces for the tangential force (as in Fig. 5) and the differential displacement for the case of gross slip of the contact between the two vibrating samples. The master sample is driven by at 84 Hz, and it vibrates harmonically with an amplitude of ≈100 μm peak to peak. Bottom trace is the corresponding displacement waveform (amplitude ≈20 μm peak to peak). (b) Plot of the tangential force–differential displacement revealing the hysteresis.

84 Hz, but this has no consequence in the development of the experiment. The measured vibration has a differential amplitude of 20 μm peak to peak, and has a distorted sine wave. The common-mode vibration of the master sample had an approximately 100 μm peak-to-peak amplitude. When the tangential force is plotted versus the differential vibration for a single period of the vibration, the hysteresis cycle shown in Fig. 8(b) is obtained. The study of a sequence of single-shot hysteresis cycles is important because trajectories can vary from cycle to cycle and can also depend on the wear of the contact and on its temperature.

Another important application is the measurement of the hysteresis cycle when the samples are kept at high temperature 700–900 °C, that is, in a condition closely approaching that occurring in a turbine engine. The SMI vibrometer performed well for the high-temperature application, where other conventional laser vibrometers may fail due to the large background noise caused by the blackbody emission of the targets.

4. Conclusions

We have presented the development of a noncontact differential laser vibrometer for application to the characterization of vibrating contacts between two samples in the presence of friction damping in the microslip and gross-slip regimes. The approach based on the electronic difference of signals from two distinct half-fringe stabilized SMI has proved to be successful. Operation was at a substantial distance (400 mm typically) on untreated diffusing surfaces for the target and achieved a submicrometer sensitivity for the differential vibration amplitude superposed to an ≈100 μm common-mode vibration amplitude. The prototype has been successfully tested on a purposely developed test rig, and hysteresis cycles have been measured for the microslip and gross-slip regimes.

The authors thank Muzio Gola and Sergio Filippi (Department of Mechanics, Politecnico di Torino) for kindly supplying the results of the SMI measurements on their mechanical apparatus and for the useful discussions on the applicability of the optical techniques.

References

1. S. Donati, *Electro-Optical Instrumentation—Sensing and Measuring with Lasers* (Prentice Hall, 2004).
2. G. Giuliani, M. Norgia, S. Donati, and T. Bosch, "Laser diode self-mixing technique for sensing applications," J. Opt. A **4,** S283–S294 (2002).
3. S. Donati, G. Giuliani, and S. Merlo, "Laser diode feedback interferometer for measurement of displacements without ambiguity," IEEE J. Quantum Electron. **31,** 113–119 (1995).
4. M. Norgia, S. Donati, and A. D'Alessandro, "Interferometric measurement of displacement on a diffusing target by a speckle tracking technique," IEEE J. Quantum Electron. **37,** 800–806 (2001).
5. M. Norgia and S. Donati, "A displacement measuring Instrument utilizing self-mixing inteferometry," IEEE Trans. Instrum. Meas. **52,** 1765–1769 (2003).
6. F. Gouaux, N. Servagent, and T. Bosch, "Absolute distance measurement with an optical feedback interferometer," Appl. Opt. **37,** 6684–6689 (1998).
7. G. Giuliani, S. Bozzi-Pietra, and S. Donati, "Self-mixing laser diode vibrometer," Meas. Sci. Technol. **14,** 24–32 (2003).
8. N. Servagent, T. Bosch, and M. Lescure, "A laser displacement sensor using the self-mixing effect for modal analysis and defect detection," IEEE Trans. Instrum. Meas. **46,** 847–850 (1997).
9. G. Giuliani, S. Donati, M. Passerini, and T. Bosch, "Angle measurement by injection detection in a laser diode," Opt. Eng. **40,** 95–99 (2001).
10. J. H. Griffin, "A review of friction damping of turbine blade vibration," Int. J. Turbo Jet Eng. **7,** 297–307 (1990).
11. A. V. Srinivasan, "Flutter and resonant vibration characteristics of engine blades," J. Eng. Gas Turbines Power **119,** 742–775 (1997).
12. S. Filippi, A. Akay, and M. M. Gola, "Measurement of tangential contact hysteresis during microslip," J. Tribol. **126,** 482–489 (2004).